# Analysis of Catalytic Carboxylate Mutants E552Q and E1197Q Suggests Asymmetric ATP Hydrolysis by the Two Nucleotide-Binding Domains of P-Glycoprotein[†]

Isabelle Carrier, Michel Julien,[‡] and Philippe Gros*

*Department of Biochemistry and McGill Cancer Centre, McGill University, Montréal, Québec, Canada H3G 1Y6*

*Received February 18, 2003; Revised Manuscript Received August 14, 2003*

ABSTRACT: In the nucleotide-binding domains (NBDs) of ABC transporters, such as mouse Mdr3 P-glycoprotein (P-gp), an invariant carboxylate residue (E552 in NBD1; E1197 in NBD2) immediately follows the Walker B motif (hyd$_4$D**E/D**). Removal of the negative charge in mutants E552Q and E1197Q abolishes drug-stimulated ATPase activity measured by $P_i$ release. Surprisingly, drug-stimulated trapping of 8-azido-[α-$^{32}$P]ATP is still observed in the mutants in both the presence and absence of the transition-state analogue vanadate ($V_i$), and ADP can be recovered from the trapped enzymes. The E552Q and E1197Q mutants show characteristics similar to those of the wild-type (WT) enzyme with respect to 8-azido-[α-$^{32}$P]ATP binding and 8-azido-[α-$^{32}$P]nucleotide trapping, with the latter being both $Mg^{2+}$ and temperature dependent. Importantly, drug-stimulated nucleotide trapping in E552Q is stimulated by $V_i$ and resembles the WT enzyme, while it is almost completely $V_i$ insensitive in E1197Q. Similar nucleotide trapping properties are observed when aluminum fluoride or beryllium fluoride is used as an alternate transition-state analogue. Partial proteolytic cleavage of photolabeled enzymes indicates that, in the absence of $V_i$, nucleotide trapping occurs exclusively at the mutant NBD, whereas in the presence of $V_i$, nucleotide trapping occurs at both NBDs. Together, these results suggest that there is single-site turnover occurring in the E552Q and E1197Q mutants and that ADP release from the mutant site, or another catalytic step, is impaired in these mutants. Furthermore, our results support a model in which the two NBDs of P-gp are not functionally equivalent.

The successful chemotherapeutic treatment of many human tumors is often impeded by the emergence of multidrug-resistant cells (*1*). Multidrug resistance (MDR)[1] is characterized by cross-resistance to structurally and functionally unrelated compounds and is often associated with the overexpression of membrane transporters of wide substrate specificity, such as members of the ATP-binding cassette (ABC) protein superfamily, which include P-glycoprotein (P-gp), multidrug resistance-associated protein (MRP), and breast cancer resistance protein (BCRP) (*2*). ABC transporters form one of the largest and most conserved gene families known, with 48 members in humans, 56 in the fly, 129 in plants, and over 300 in bacteria (*3*). In humans, multiple sequence alignments divide these trans-

porters into 7 subfamilies designated ABCA to ABCG. There is great clinical interest in ABC transporters not only because of their involvement in multidrug resistance but also because many disease-causing mutations have been identified in proteins of this family in humans, causing diseases such as Tangier disease (ABCA1), progressive intrahepatic cholestasis (ABCB11), pseudoxanthoma elasticum (ABCC6), cystic fibrosis (ABCC7), persistent hyperinsulinemic hypoglycemia (ABCC8), adrenoleukodystrophy (ABCD1), and sitosterolemia (ABCG5, ABCG8) among others. The substrates for ABC transporters are very diverse and include drugs (ABCB1), lipids (ABCA4, ABCA7, ABCB4), fatty acids (ABCD1−4), sterols (ABCG5, ABCG8), anionic conjugates (ABCC1−3), peptides (ABCB2, ABCB3), nucleotides (ABCC4, ABCC5), and ions (ABCB6, ABCB7, ABCC7) (http://humanabc.4t.com/humanabc.htm), which are all transported across the phospholipid bilayer at the expense of ATP (*3*).

ABC transporters are defined by a structural unit composed of six putative transmembrane α-helices that form one transmembrane domain (TMD) and one cytosolic nucleotide-binding domain (NBD) (*4*, *5*). In prokaryotes, the TMDs and NBDs are most often encoded by separate structural genes of the same operon (*6*). In eukaryotes, many ABC transporters, including P-gp, show a duplication of this unit in a single polypeptide, while others appear to function as homo- or heterodimers of the 1TMD/1NBD unit (TAP1/2, ABCB2/3, ABCG5/8). Also, members of the ABCC subfamily (MRP,

SUR1) show an additional hydrophobic domain of five TM helices fused at the N-terminus of the classical 2TMD/2NBD backbone. The major topological features of P-gp, including the carboxy and amino termini, the glycosylated loop, and the NBDs, have been oriented with respect to the cell membrane, and the number, position, and polarity of the 12 TM helices have been established using biochemical and immunological methods (*7, 8*). Recently, a high-resolution structure was obtained for the ABC transporter MsbA (homodimer, 1TMD/1NBD) of *Escherichia coli* (*E. coli*) (*9*), which confirmed at 6 the number of TM helices present in each TMD of ABC transporters. Peptide mapping with photoactive substrate analogues (*10*) and studies in chimeric (*11, 12*), naturally occurring (*13, 14*), or experimentally induced (*15, 16*) P-gp mutants with altered substrate specificities, as well as site-specific modifications in single-cysteine mutants (*17*), suggest that the TMDs of P-gp, and of other ABC transporters, form the substrate-binding site in the lipid bilayer.

Drug transport is strictly ATP dependent, and considerable evidence suggests that ATP hydrolysis by the NBDs provides the energy required for this process (*18−23*). Purified P-gp shows robust ATPase activity [measured by the release of inorganic phosphate ($P_i$) or by vanadate- ($V_i$-) induced trapping of nucleotide] that can be further stimulated by certain MDR drugs and P-gp inhibitors (*18, 19, 21, 24*). Both NBDs have been shown, through mutagenesis (*25*), site-specific modification in single-cysteine mutants (*26*), and studies in half-molecules (*27*), to be essential for function, with complete cooperativity between the two sites for ATP hydrolysis and drug transport. In the "alternate site" catalysis model proposed by Senior and co-workers (*22*), both NBDs are catalytically active with equal probability of hydrolysis at NBD1 and NBD2. In this model, one drug molecule is transported per ATP molecule hydrolyzed. The experiments that support this model include $V_i$-induced nucleotide trapping, in which equal trapping of nucleotide occurs in NBD1 and NBD2, with complete inhibition of ATPase activity occurring with one molecule of $V_i$ trapped per P-gp molecule (*28, 29*). Thus, when one site enters the transition state (P-gp·MgADP·$P_i$/$V_i$), the other cannot do so, implying alternate hydrolysis. In the expanded model proposed by Ambudkar and co-workers, two ATP molecules need to be hydrolyzed for one substrate molecule to be transported (*30*). This model is based on the observations that $V_i$-inhibited P-gp has reduced affinity for drugs (*30−32*) and that a second ATP hydrolysis event is required to restore normal drug-binding properties (*30*). Hence, drug binding induces hydrolysis of a first ATP and translocation of substrate to a low-affinity site, as well as substrate release, while binding and hydrolysis of a second ATP is required to recreate a high-affinity drug-binding site.

In ABC proteins, each NBD contains the consensus Walker A ($GX_4GKS/T$) and Walker B ($hyd_4D$, where hyd = hydrophobic residue) sequence motifs that have been previously described in various ATP-binding proteins and ATP-hydrolyzing enzymes (ATPases) (*33*). The high-resolution crystal structures of several NBDs of ABC transporters and proteins have been solved, including HisP, MalK, MJ0796 (LolD), MJ1267 (LivG), Rad50cd, TAP1, BtuCD, and HlyB (*34−41*). In most cases, structural information has been obtained for the protein bound to different nucleotides,

revealing the location of the nucleotide complexes and defining the amino acid residues that form the active site. For example, the Walker A motif, also known as the P-loop, is seen to wrap around the phosphate chain of ATP with the main chain nitrogens of the residues within this motif making extensive hydrogen bonding with the $\beta$-phosphate. The Walker B motif is shown to provide the carboxylate residue that coordinates and stabilizes the magnesium ion indispensable for ATP hydrolysis. In addition, the recent crystal structure of the stable MJ0796-E171Q dimer (*42*) shows that the signature motif of the opposite NBD also contributes to the active site by forming hydrogen bonds with the ribose and $\gamma$-phosphate of ATP. Finally, multiple sequence alignments identified another highly conserved carboxylate residue that immediately follows the Walker B aspartate (*43*). This carboxylate has been proposed to play a key role in catalysis since, in the HisP structure, the negatively charged side chain of this glutamate (E179) appears to polarize a water molecule for an in-line attack on the terminal phosphate of ATP (*34*).

In an effort to gain insight into the mechanism of ATP hydrolysis by P-gp, including testing the role of the two NBDs in catalysis, we have previously mutated the glutamate residues homologous to E179 of HisP in the mouse Mdr3 enzyme (E552Q and E1197Q in NBD1 and NBD2, respectively) (*43*). We observed that although no ATPase activity could be measured by $P_i$ release for either of these mutants, 8-azido-[$\alpha$-$^{32}$P]nucleotide could still be trapped. These observations have suggested that a step during ATP hydrolysis is impaired in the mutant enzymes, providing a unique opportunity to study intermediate steps in the catalytic cycle of the enzyme. In this study, we have attempted to characterize the molecular basis of the defect in the E552Q and E1197Q mutants.

## EXPERIMENTAL PROCEDURES

*Purification of Mouse Mdr3.* The wild-type mouse Mdr3 (WT) and the E552Q, E1197Q, and D551N mutants were created by site-directed mutagenesis and modified by in-frame addition of a six-histidine tag ($His_6$) at the C-terminus of the protein and were expressed in the yeast *Pichia pastoris* after cloning in the expression plasmid pHIL-D2 (Invitrogen, license 145457), as previously described (*43*). For expression and purification, glycerol stocks of *P. pastoris* GS115 transformants were streaked on YPD plates, and single colonies were used to inoculate 6 L liquid cultures. For preparation of *P. pastoris* membranes, cultures were induced with 1% methanol for 72 h, and plasma membranes were isolated by centrifugation, as previously described (*44*). Solubilization and purification of WT and mutant Mdr3 variants by affinity chromatography on Ni-NTA resin (Qiagen) and DE52-cellulose (Whatman) were as described (*44*). This procedure routinely yielded between 1 and 1.6 mg of protein, with 95% minimum purity.

*Assay of ATPase Activity.* For ATPase assays, purified WT or mutant Mdr3 enzymes (concentrated DE52 eluate) were activated by incubating with 1% *E. coli* lipids (w/v; Avanti, acetone/ether preparation) and 5 mM dithiothreitol (DTT) for 30 min at 20 °C at a final protein concentration of 0.07 $\mu$g/$\mu$L (WT) or 0.1 $\mu$g/$\mu$L (mutants). Aliquots of 5 $\mu$L were added into 50 mM Tris-HCl (pH 8.0), 0.1 mM EGTA, 10 mM $Na_2$ATP, and 10 mM $MgCl_2$, to a final volume of 250

$\mu$L, and the mixture was incubated at 37 °C. At the appropriate time, a 50 $\mu$L aliquot was removed and quenched in 1 mL of ice-cold 20 mM $H_2SO_4$. Inorganic phosphate ($P_i$) release was assayed as described previously (*45*). Drugs were added as dimethyl sulfoxide stock solutions, and the final solvent concentration in the assay was kept at ≤2% (v/v).

*Photoaffinity Labeling with 8-Azido-[$\alpha$-$^{32}$P]ATP.* 8-Azido-[$\alpha$-$^{32}$P]ATP photoaffinity labeling was performed as previously described (*43*) with minor modifications. The purified Mdr3 proteins (concentrated DE52 eluate) were activated by incubating with 1% *E. coli* lipids (w/v; Avanti, acetone/ether preparation) and 5 mM DTT at a final concentration of 0.2 mg/mL at 20 °C for 30 min immediately prior to starting the photolabeling reactions. For direct labeling experiments, activated WT or mutant Mdr3 variants were incubated on ice for ~10 min with 3 mM $MgCl_2$, 50 mM Tris-HCl (pH 8.0), 0.1 mM EGTA, and varying concentrations of 8-azido-[$\alpha$-$^{32}$P]ATP (5, 10, 20, 40, and 80 $\mu$M final concentrations at ~0.2 Ci/mmol specific activity) in a total volume of 50 $\mu$L. In some experiments, requirement for divalent cations was assayed by addition of EDTA (5 mM) to the reaction mixture. The samples were kept on ice and immediately UV-irradiated for 5 min [UVS-II Minerallight (260 nm) placed directly above the samples]. Unreacted nucleotides were then removed by centrifugation at 200000$g$ for 30 min at 4 °C in a TL-100 rotor (Beckman), and protein-containing pellets were washed with 100 $\mu$L of ice-cold 50 mM Tris-HCl (pH 8.0) and 0.1 mM EGTA. The pellets were then dissolved in sample buffer [5% (w/v) SDS, 25% (v/v) glycerol, 0.125 M Tris-HCl (pH 6.8), 40 mM DTT, 0.01% pyronin Y] and separated by SDS–polyacrylamide gel electrophoresis (SDS–PAGE) on 7.5% gels, followed by autoradiography to Kodak BioMax MS film. For nucleotide trapping experiments, activated WT or mutant Mdr3 variants were incubated at 37 °C for 20 min with 5 $\mu$M 8-azido-[$\alpha$-$^{32}$P]ATP (0.2–0.5 Ci/mmol), 3 mM $MgCl_2$, 50 mM Tris-HCl (pH 8.0), and 0.1 mM EGTA, with or without vanadate ($V_i$, 200 $\mu$M), $AlCl_3$ (1 mM)–NaF (5 mM), or $BeSO_4$ (200 $\mu$M)–NaF (1 mM), in a total volume of 50 $\mu$L. Verapamil (100 $\mu$M) or valinomycin (100 $\mu$M) was included where indicated. Divalent cation dependence was assayed by addition of EDTA (5 mM). Modifications to the normal procedure are indicated in the figure legends. The incubations were started by addition of 8-azido-[$\alpha$-$^{32}$P]ATP and stopped by transfer on ice. Free label was then removed by centrifugation at 200000$g$ for 30 min at 4 °C in a TL-100 rotor (Beckman), and pellets were washed and resuspended in 30 $\mu$L of ice-cold 50 mM Tris-HCl (pH 8.0) and 0.1 mM EGTA. Samples were kept on ice and irradiated with UV for 5 min. Labeled samples were resolved by SDS–PAGE on 7.5% gels and subjected to autoradiography. Orthovanadate solutions (100 mM) were prepared from $Na_3VO_4$ (Fisher Scientific) at pH 10 and boiled for 2 min before use to break down polymeric species.

*Thin-Layer Chromatography Analysis of Vanadate-Trapped Nucleotides in Mouse Mdr3.* Five micrograms of activated WT or mutant Mdr3 variants was incubated at 37 or 4 °C for 10 min with 5 $\mu$M 8-azido-[$\alpha$-$^{32}$P]ATP (0.4 Ci/mmol), 3 mM $MgCl_2$, 200 $\mu$M vanadate, 100 $\mu$M verapamil, 50 mM Tris-HCl (pH 8.0), and 0.1 mM EGTA in a total volume of 50 $\mu$L. The incubations were started by addition of 8-azido-[$\alpha$-$^{32}$P]ATP and stopped by transfer on ice. The free label was removed by centrifugation at 200000$g$ for 30 min at 4 °C in a TL-100 rotor (Beckman), and the pellets were washed with ice-cold 50 mM Tris-HCl (pH 8.0) and 0.1 mM EGTA. The protein pellets were then resuspended in 15 $\mu$L of 50 $\mu$M 8-azido-ATP, and 2 $\mu$L of ice-cold 50% (w/v) trichloroacetic acid was added. The samples were centrifuged to precipitate the protein, and 1 $\mu$L of 50 mM EDTA was added to 20 $\mu$L of the supernatant. Samples (0.5 $\mu$L) were applied to a poly(ethylenimine)−cellulose plate along with 125 dpm of each nucleotide standard (8-azido-ATP, 8-azido-ADP, and a mixture of both ± protein) and developed in 3.2% (w/v) fresh $NH_4HCO_3$; the plate was then subjected to autoradiography.

*Partial Trypsin Digestion of Photolabeled Mouse Mdr3.* To detect radiolabeled nucleotide trapped in NBD1 and/or NBD2 of Mdr3 following photolabeling of the protein with 8-azido-[$\alpha$-$^{32}$P]ATP, we took advantage of the protease-hypersensitive site located in the linker region joining the two halves of P-gp (*46*). Photoaffinity-labeled proteins were resuspended in 30 $\mu$L of 50 mM Tris-HCl (pH 8.0) and 0.1 mM EGTA and kept on ice. The incubation with trypsin (2 $\mu$L of each stock solution) was then carried out for 10 min at 37 °C at enzyme-to-protein mass ratios of 1:75, 1:37.5, 1:18.75, 1:9.38, 1:4.69, 1:2.34, and 1:1.17. The digestion was stopped by addition of 15 $\mu$L of sample buffer. For the experiment carried out in the absence of $V_i$ all ratios were used, whereas in the presence of $V_i$ only the 1:37.5, 1:18.75, 1:9.38, and 1:4.69 ratios were used. Finally, the Mdr3 halves were resolved by SDS−PAGE on 10% gels, followed by transfer onto nitrocellulose membranes and exposition to film. Immunoblotting with the mouse monoclonal antibody C219 (Signet) that recognizes both halves of Mdr3, as well as with N-terminal and C-terminal half specific mouse monoclonal antibodies [MD13 with its epitope in NBD1 (494−504) and MD7 with its epitope in the intracellular (IC) loop 3 (805−815)], respectively (gift of Dr. V. Ling from The B.C. Cancer Research Centre, Vancouver, Canada) (*47*), was then performed on the membranes.

*Routine Procedures.* Protein concentrations were determined by the bicinchoninic acid method in the presence of 0.5% SDS using bovine serum albumin as a standard. SDS−PAGE was carried out according to Laemmli (*48*) using the mini-PROTEAN II gel and Electrotransfer system (Bio-Rad). Samples were dissolved in sample buffer [5% SDS (w/v), 25% glycerol (v/v), 125 mM Tris-HCl (pH 6.8), 40 mM DTT, and 0.01% pyronin Y]. For immunodetection of Mdr3, the mouse monoclonal antibody C219 (Signet Laboratories Inc.) was used with the enhanced chemiluminescence (ECL) detection system (NEN Renaissance, PerkinElmer). To recognize NBD1 specifically, the mouse monoclonal antibody MD13 was used, and for NBD2 the mouse monoclonal antibody MD7 was employed. For autoradiography, SDS gels were stained with Coomassie Blue, dried, and exposed at −80 °C to Kodak BioMax MS film with an intensifying screen for the appropriate amount of time.

*Materials.* 8-Azido-[$\alpha$-$^{32}$P]ATP was purchased from Affinity Labeling Technologies, Inc. (Lexington, KY). 8-Azido-ATP and verapamil were from ICN while valinomycin was from Calbiochem. Acetone/ether-precipitated *E. coli* lipids were from Avanti Polar Lipids. The PEI−cellulose TLC plates and general reagent grade chemicals were from Sigma or Fisher.
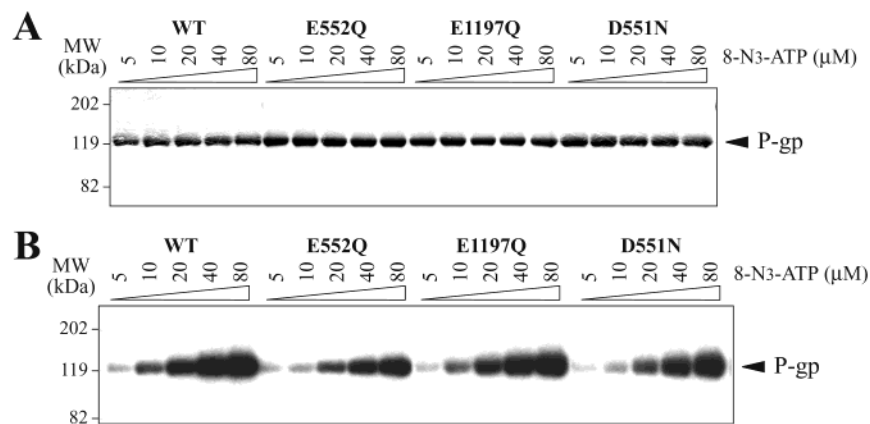
FIGURE 1: Direct photolabeling of purified Mdr3 NB site mutants with Mg-8-azido-[α-$^{32}$P]ATP. Purified and activated wild-type (WT) and mutant Mdr3 variants (E552Q, E1197Q, D551N) were UV-irradiated on ice in the presence of 3 mM MgCl$_2$ and 5, 10, 20, 40, and 80 μM 8-azido-[α-$^{32}$P]ATP. Photolabeled samples were separated on 7.5% SDS–polyacrylamide gels and stained with Coomassie Blue (A) followed by autoradiography (B) (Experimental Procedures). The position of the molecular mass markers is given on the left.

## RESULTS

During a previous search for catalytic carboxylate residues in the NBDs of P-glycoprotein two mutants of the mouse Mdr3 isoform at homologous positions in NBD1 and NBD2 (E552Q and E1197Q) showed a similar loss-of-function phenotype, which featured inability to convey multidrug resistance and abrogation of steady-state ATPase activity (*43*). In the present study, we have investigated the mechanistic basis of the defect in those mutants. For this, wild-type (WT) Mdr3 and the E552Q and E1197Q mutants were expressed in the yeast *P. pastoris* as recombinant proteins bearing an in-frame polyhistidine tail (His$_6$) at the carboxyl terminus. The NBD1 Walker B motif mutant D551N, in which ATP hydrolysis is completely impaired [*49, 50* (*hMDR1*)], was also included as a negative control in the experiments. Protein purification from large-scale methanol-induced liquid cultures of *P. pastoris* was done by detergent extraction from enriched membrane fractions, followed by affinity and anion-exchange chromatography on Ni$^{2+}$-NTA and DE52-cellulose resins, respectively (*44*). Using this protocol, all proteins could be purified in large amounts (1–1.6 mg/6 L culture) in a stable form and at a high degree of purity (>95%) (Figure 1A).

Steady-state ATP hydrolysis by the purified proteins activated with *E. coli* lipids and DTT was determined by measuring P$_i$ release, in the absence or presence of MDR drugs or P-gp inhibitors that are known to stimulate the ATPase activity of P-gp (*45*). As shown previously (*43*), WT Mdr3 has low basal ATPase activity (0.35 μmol min$^{-1}$ mg$^{-1}$), which can be strongly stimulated (6–9-fold) by verapamil and valinomycin (3.16 and 2.18 μmol min$^{-1}$ mg$^{-1}$). As before, the purified E552Q and E1197Q mutants show a very low basal ATPase activity (0.13–0.18 μmol min$^{-1}$ mg$^{-1}$) that is not stimulated by drugs (0.13–0.20 μmol min$^{-1}$ mg$^{-1}$) and which is comparable to the activity seen in the ATPase inactive mutant D551N (*49, 51*) that is considered to be background.

To determine whether the loss of ATPase activity seen in E552Q and E1197Q was caused by an effect of the mutations on affinity for nucleotides, the nucleotide-binding properties of the WT and Mdr3 variants were compared by photoaffinity labeling. Purified and activated proteins were incubated with increasing concentrations of 8-azido-[α-$^{32}$P]ATP in the presence of Mg$^{2+}$ (∼10 min on ice), followed by UV irradiation. Unincorporated ligand was removed by centrifugation, and labeled proteins were resolved by SDS–PAGE. The gels were stained with Coomassie Blue to verify comparable loading (Figure 1A) and then subjected to autoradiography (Figure 1B). Binding and subsequent photo-cross-linking of 8-azido-[α-$^{32}$P]ATP was specific to Mdr3 and increased proportionally with the amount of 8-azido-[α-$^{32}$P]ATP present in the reaction. The profile of $^{32}$P incorporation over several experiments was quantitatively similar for all mutants and was also very similar to that seen for WT Mdr3. Similar results were obtained when the WT and mutant proteins were labeled at 4 °C with 8-azido-[γ-$^{32}$P]ATP (data not shown). Together, these results suggest that the E552Q, E1197Q, and D551N mutations do not have a major effect on nucleotide binding to Mdr3 and are therefore unlikely to cause major nonspecific structural changes in the NBDs. This is in agreement with previous studies of catalytic residue mutants of the Walker A and B signature motifs (K429R, K1072R, D551N, and D1196N) which severely affect the catalytic activity of mouse Mdr3 but have little effect on the nucleotide-binding affinity of the protein (*49*). Thus, residues E552 and E1197 seem to participate in the hydrolysis steps after the initial binding of ATP to the NBDs.

Vanadate (V$_i$) is a transition-state analogue structurally related to phosphate (P$_i$) that can stably inhibit P-gp ATPase activity (*52*). V$_i$ trapping of nucleotide requires both hydrolysis of the bond between the β- and γ-phosphates of ATP and release of P$_i$. Once P$_i$ is released, it is replaced by V$_i$, capturing ADP in the NB site and forming a long-lived intermediate that resembles the normal transition state {MgADP·V$_i$} (*28*). This intermediate can be visualized by UV cross-linking when 8-azido-[α-$^{32}$P]ATP is used as a substrate (*28*). Indeed, V$_i$-induced trapping of 8-azido-[α-$^{32}$P]ADP under hydrolysis conditions (37 °C) has been used as an alternative and highly sensitive method to monitor ATPase activity in WT and mutant P-gp (*28, 49*). For WT Mdr3, nucleotide trapping is dependent on the presence of V$_i$ and is stimulated by VER and VAL. In contrast to WT, nucleotide trapping is completely absent from the Walker B
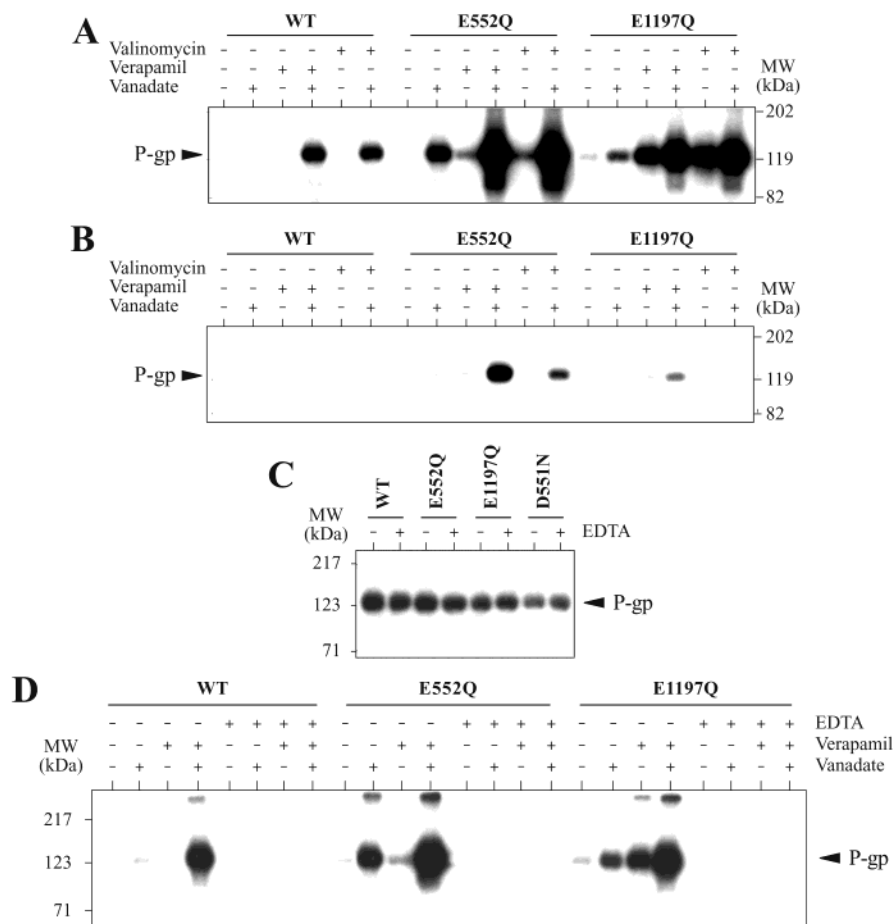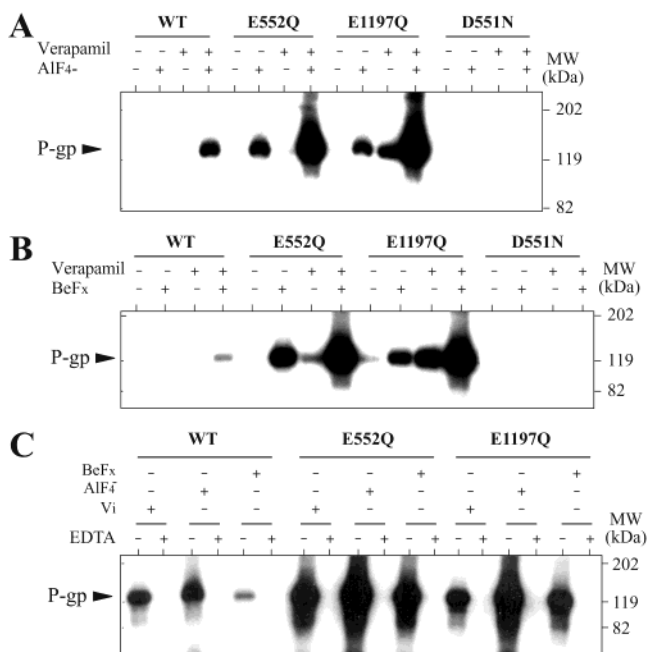
FIGURE 2: Temperature and divalent cation dependence of photolabeling of Mdr3 NB site mutants by vanadate trapping with Mg-8-azido-[$\alpha$-$^{32}$P]ATP. Purified and activated wild-type and mutant Mdr3 variants were preincubated with 5 $\mu$M 8-azido-[$\alpha$-$^{32}$P]ATP and 3 mM MgCl$_2$ for 20 min at either 37 °C (A and D) or on ice (4 °C; B) in the absence or presence of 200 $\mu$M vanadate, 100 $\mu$M verapamil or 100 $\mu$M valinomycin, and 5 mM EDTA (D only), as indicated above the lanes. Unbound ligands were removed by ultracentrifugation and washing, and the samples were then UV-irradiated and separated by SDS−PAGE. The autoradiographs in panels A and B were exposed to film for the same amount of time. (C) Purified and activated wild-type and mutant P-gp variants were UV-irradiated on ice in the presence of 20 $\mu$M 8-azido-[$\alpha$-$^{32}$P]ATP and 3 mM MgCl$_2$, with or without 5 mM EDTA, as indicated above the lanes. Photolabeled samples were separated on 7.5% SDS−polyacrylamide gels and stained with Coomassie Blue followed by autoradiography.

mutant D551N under any of the conditions tested, as suggested by the absence of ATPase activity of this mutant. Despite the observed lack of ATPase activity of E552Q and E1197Q measured by P$_i$ release, 8-azidonucleotide trapping that is stimulated both by drug and by V$_i$ is readily detectable in these mutants. Interestingly, drug-stimulated V$_i$-independent trapping is also seen in the mutants. We proposed previously that these mutants can only complete part of the ATP hydrolysis cycle of P-gp, such that binding of 8-azido-ATP and initiation of hydrolysis leading to formation of the transition-state complex are normal, but subsequent steps, such as release of MgADP and/or P$_i$, or others are impaired (*43*).

Although studies of WT Mdr3 [Figure 1 and (*43*)] and of the inactive mutant D551N [Figure 1 and (*43*)] suggest that under the hydrolysis conditions used (37 °C; see Experimental Procedures) little if any of the photolabeling is due to 8-azido-[$\alpha$-$^{32}$P]ATP binding, additional experiments were undertaken to verify that the labeling seen in E552Q and E1197Q ($\pm$V$_i$) was due to trapping of hydrolyzed nucleotide, as opposed to simple binding of the label to Mdr3. As formation of the Mg-8-azido-ADP·V$_i$ complex is optimum at 37 °C and requires Mg$^{2+}$ ions (*28*, *53*), the

temperature dependence and EDTA sensitivity of E552Q and E1197Q photolabeling by 8-azido-[$\alpha$-$^{32}$P]ATP were investigated. Results in Figure 2A,B show that labeling of WT, E552Q, and E1197Q by 8-azido-[$\alpha$-$^{32}$P]ATP under all conditions tested ($\pm$V$_i$, $\pm$drugs) was either completely eliminated or largely reduced (>90%) when the incubation and washing steps of the labeling reaction were carried out at 4 °C (Figure 2B) as opposed to 37 °C (Figure 2A). Parallel studies of Mg$^{2+}$ ion dependence of 8-azido-[$\alpha$-$^{32}$P]ATP labeling under hydrolysis conditions, shown in Figure 2D, indicate that addition of the chelator EDTA completely abrogates photolabeling of the WT and mutant proteins, under all conditions tested ($\pm$V$_i$, $\pm$drugs). On the other hand, addition of EDTA to the reaction mixture is without effect on labeling of WT and mutant variants under nucleotide-binding conditions (4 °C; see Experimental Procedures) (Figure 2C), in agreement with previous studies showing that nucleotide binding to P-gp is largely Mg$^{2+}$ independent (*44*, *50*). These results are consistent with 8-azido-[$\alpha$-$^{32}$P]ATP hydrolysis in the WT and E552Q and E1197Q mutants with concomitant trapping of 8-azido-[$\alpha$-$^{32}$P]ADP. The differences in signal intensity that can be observed for the WT protein in the presence of vanadate

**FIGURE 3:** Photolabeling of Mdr3 NB site mutants by aluminum fluoride and beryllium fluoride trapping with Mg-8-azido-[α-³²P]-ATP. Purified and activated wild-type and mutant Mdr3 variants were preincubated for 20 min at 37 °C with 5 μM 8-azido-[α-³²P]-ATP and 3 mM MgCl₂ in the absence or presence of 100 μM verapamil, 1 mM aluminum chloride, and 5 mM sodium fluoride (A; AlF₄⁻) or 0.2 mM beryllium sulfate and 1 mM sodium fluoride (B; BeF$_x$), as indicated above the lanes. Samples were processed for photolabeling as described in Experimental Procedures and analyzed by SDS−PAGE. (C) The EDTA sensitivity of AlF₄⁻, BeF$_x$, and vanadate (V$_i$) induced trapping of nucleotide in WT and mutant Mdr3 variants was tested as described in the legend to Figure 2. The gel in (C) was overexposed to ascertain the absence of labeling in all +EDTA lanes.

and in the absence of drug between different experiments are likely due in part to different times of exposure and also to small differences in experimental conditions (such as different protein preparations).

To obtain further evidence that the E552Q and E1197Q mutants can form the {MgADP·V$_i$} transition-state complex, similar nucleotide trapping experiments were carried out in the presence of two other transition-state analogues: aluminum fluoride (AlF₄⁻) and beryllium fluoride (BeF$_x$). Crystallographic studies of the myosin motor domain from *Dictyostelium discoideum* complexed to these P$_i$ analogues show that the V$_i$- and AlF₄⁻-inhibited complexes are very similar and display a bond length of 2.0 Å between the V or Al atom and the pseudo-bridging oxygen (O) of the β-phosphorus of ADP. This bond length is significantly longer than the 1.56 and 1.67 Å bond lengths for the O atoms between the α- and β-phosphate groups of ADP, an observation strongly supporting the proposal that MgADP·V$_i$ and MgADP·AlF₄⁻ complexes are true analogues of the MgADP·P$_i$ transition state. On the other hand, the bond length measured for the Be to βO bond in the MgADP·BeF$_x$-inhibited complex is 1.57 Å, which is very similar to that seen for the P−O bond linking the α- and β-phosphates. This indicates that the MgADP·BeF$_x$ complex more closely resembles ATP bound in the active site, reflecting the ground state of the enzyme prior to hydrolysis (*54, 55*). Results in Figure 3A indicate that AlF₄⁻ can also induce nucleotide trapping in the WT and E552Q and E1197Q mutants, with
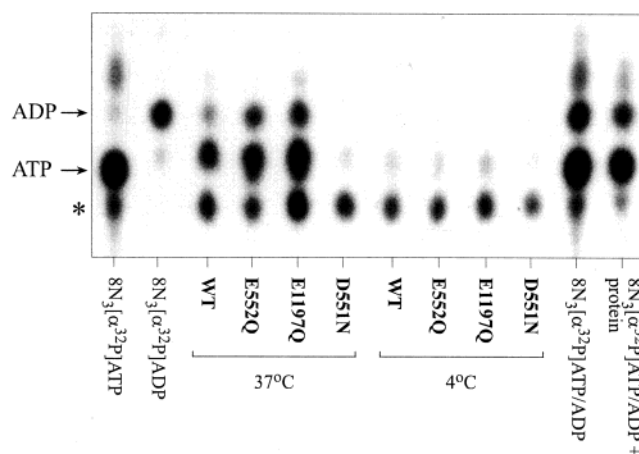


**FIGURE 4:** Thin-layer chromatography analysis of vanadate-trapped nucleotides in Mdr3 NB site mutants. Purified and activated wild-type and mutant Mdr3 variants were preincubated with 5 μM 8-azido-[α-³²P]ATP and 3 mM MgCl₂ for 10 min at either 37 or 4 °C in the presence of 200 μM vanadate and 100 μM verapamil. Unbound ligands were removed by ultracentrifugation and washing. The protein pellets were then resuspended in 8-azido-ATP and precipitated by TCA. The supernatant (0.5 μL) and 125 dpm of standards were applied to a PEI−cellulose plate following magnesium chelation with EDTA. The plate was developed in 3.2% (w/v) NH₄HCO₃ and exposed to film. The asterisk (*) indicates the position of a nonspecific radioactive contaminant present in the commercial preparation of 8-azido-[α-³²P]ATP.

characteristics similar to those observed when V$_i$ is used to induce trapping (*43*). BeF$_x$ can also induce nucleotide trapping in the WT and mutant Mdr3 enzymes (Figure 3B). On the other hand, neither BeF$_x$ nor AlF₄⁻ could induce nucleotide trapping in the inactive Walker B mutant D551N (Figure 3A,B), in agreement with the V$_i$-induced trapping data (*43*). These results show that the different transition states revealed by distinct P$_i$ analogues can all be formed in the E552Q and E1197Q mutants in a comparable manner to WT Mdr3. Finally, results in Figure 3C show that BeF$_x$- and AlF₄⁻-induced nucleotide trapping in the WT and E552Q and E1197Q mutants is EDTA sensitive. Together, these results expand observations with V$_i$ [Figure 3 (*43*)], showing that in the mutants E552Q and E1197Q activation and cleavage of the bond between the β- and γ-phosphates of ATP seem to take place.

Additionally, thin-layer chromatography (TLC) was used to identify the nucleotides bound to the enzymes following trapping in the presence of V$_i$. As seen in Figure 4, 8-azido-[α-³²P]ADP can be detected following incubation of the WT and E552Q and E1197Q mutants with 8-azido-[α-³²P]ATP and vanadate, while it is absent in the catalytically inactive D551N mutant. Furthermore, formation of ADP does not occur in any of the enzymes when the trapping reaction is carried out at 4 °C. Thus, it appears that the E552Q and E1197Q mutants are able to hydrolyze at least one molecule of ATP. In these experiments, we also detected the presence of ATP in both WT and the E552Q and E1197Q mutants. Senior and colleagues have previously reported that only ADP could be recovered from WT protein following V$_i$-induced trapping of nucleotide (*28, 56, 57*). The reason for the apparent discrepancy has not yet been determined but could be due to different experimental procedures used to eliminate unreacted nucleotides from the incubation reaction prior to recovery and analysis of bound nucleotides. An
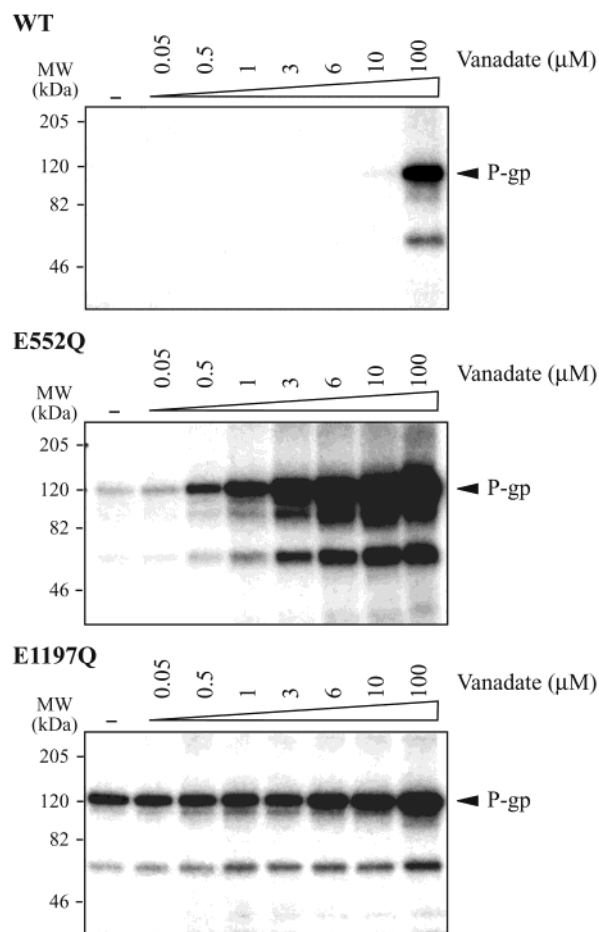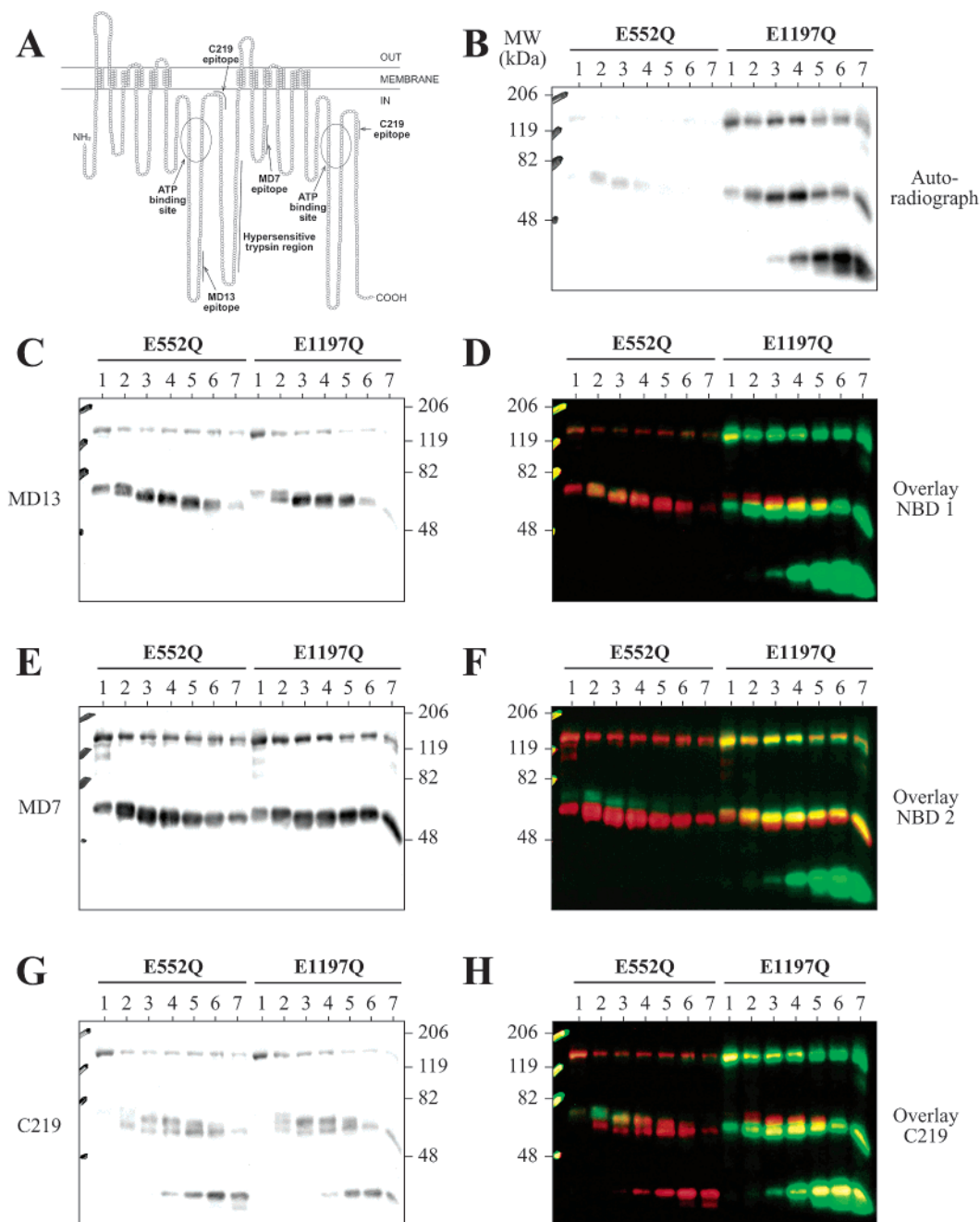
FIGURE 5: Photolabeling of Mdr3 NB site mutants with Mg-8-azido-[$\alpha$-$^{32}$P]ATP and varying concentrations of vanadate. Purified and activated wild-type and mutant Mdr3 variants were preincubated with 5 $\mu$M 8-azido-[$\alpha$-$^{32}$P]ATP, 3 mM MgCl$_2$, and 100 $\mu$M verapamil for 20 min at 37 °C in the absence or presence of increasing concentrations of vanadate, as indicated above the lanes. Samples were processed for photolabeling as described in Experimental Procedures and analyzed by SDS−PAGE.

additional radioactive spot of slower mobility is also observed in each protein-containing lane, at both 37 and 4 °C, and to a lesser extent in the diluted commercial preparation of 8-azido-[$\alpha$-$^{32}$P]ATP (Figure 4, *). The identity of this radioactive spot is currently unknown; however, its presence in all protein-containing lanes, together with the lack of temperature dependence, strongly suggests that it corresponds to a nonspecific contaminant of the commercial preparation of 8-azido-[$\alpha$-$^{32}$P]ATP that becomes slightly enriched upon incubation with protein.

The nature of the molecular defect in the E552Q and E1197Q mutants was further investigated by comparing the V$_i$ dependence of nucleotide trapping of the WT and the E552Q and E1197Q mutants in a dose−response experiment (0, 0.05 $\mu$M $\leq$ V$_i$ $\leq$ 100 $\mu$M) (Figure 5). For WT Mdr3, no trapping was observed for V$_i$ concentrations below 10 $\mu$M (K$_i$ ~5−10 $\mu$M) while robust trapping was seen at 100 $\mu$M V$_i$, a concentration known to completely inhibit P-gp ATPase activity (18−20, 24, 28). As expected from the results in our previous publication (43), both E552Q and E1197Q could trap 8-azido-[$\alpha$-$^{32}$P]nucleotide at all V$_i$ concentrations tested. However, clear differences were noted in the response of each mutant to increasing V$_i$ concentrations. E552Q showed

low levels of trapping in absence of V$_i$, but labeling increased in a dose-dependent fashion (similar to the WT enzyme) with very intense labeling seen at 100 $\mu$M V$_i$ (>50-fold stimulation). On the other hand, nucleotide trapping in E1197Q appeared to be largely V$_i$ independent, appearing robust in the absence of V$_i$ and showing only a modest increase even at the highest V$_i$ concentration tested (100 $\mu$M; 2−3-fold stimulation). The distinct V$_i$ dose−response behaviors of the two homologous mutants E552Q and E1197Q suggest that NBD1 and NBD2 are not catalytically symmetrical, with NBD2 (intact in E552Q) showing a more robust V$_i$-dependent trapping than its NBD1 counterpart (intact in E1197Q).

To further investigate a possible functional asymmetry between NBD1 and NBD2, suggested by the V$_i$ dose−response study (Figure 5), we attempted to semiquantitatively assess in which of the NBD(s) of E552Q and E1197Q the nucleotide was trapped, in both the absence and presence of V$_i$. For this, a protease-hypersensitive site present in the highly charged linker domain of the protein (46) was used to generate two Mdr3 halves that can be resolved on the gel and identified by antibodies specific for each half of the protein (Figure 6A) (58). Briefly, WT and mutant enzymes were photolabeled with 8-azido-[$\alpha$-$^{32}$P]ATP in the presence of VER to stimulate labeling, in either the absence (Figure 6) or presence (Figure 7) of V$_i$, followed by proteolytic cleavage in increasing trypsin concentrations and analysis by SDS−PAGE. The gel was then blotted onto a nitrocellulose membrane, exposed to film to reveal the $^{32}$P-labeled tryptic fragments (Figure 6B), and analyzed by immunoblotting with two monoclonal antibodies specific for the amino-terminal (MD13; Figure 6C) and carboxyl-terminal (MD7; Figure 6E) halves of the protein (47). The photolabeling signal (autoradiograph) was colorized to green, while the respective immunoblotting signals were colorized to red. Overlays of the two images are shown in panels D and F and identify in yellow the $^{32}$P photolabeled Mdr3 tryptic fragments recognized by each antibody. For E1197Q, results in panels F and H clearly show that all of the label is in the MD7-reactive, C-terminal half of the protein, with little, if any, overlap with the MD13 reactive species detected in panel D. Conversely, and although the overall photolabeling signal is much weaker than that seen for E1197Q, the label incorporated in E552Q colocalizes with the N-terminal and MD13-reactive half (panels D and H) and does not overlap with the faster migrating MD7 positive fragment (panel F). Importantly, these results show that, in the absence of V$_i$, nucleotide trapping occurs exclusively in the mutated NBD of each mutant. Although the two Mdr3 halves generated by limited trypsin digestion differ only by a few kilodaltons (62 vs 76 kDa), they can be separated by the gel system used in this and previous studies (58). This is verified (Figure 6G,H) by immunoblotting the same membrane with the monoclonal antibody C219 that recognizes a peptide epitope (VVQE/AALD) conserved in both halves of Mdr3 and present in the MD13 and MD7 immunoreactive fragments. This control also identifies the lane where the MD13 and MD7 immunoreactive fragments are present at equivalent amounts in the digest (lane 4). Because the WT protein is not labeled by 8-azido-[$\alpha$-$^{32}$P]ATP in the absence of V$_i$, it could not be analyzed in Figure 6.

FIGURE 6:  Trypsin digestion of Mdr3 NB site mutants photolabeled with Mg-8-azido-[$\alpha$-$^{32}$P]ATP in the absence of vanadate. Purified and activated mutant Mdr3 variants were preincubated with 5 $\mu$M 8-azido-[$\alpha$-$^{32}$P]ATP, 3 mM MgCl$_2$, and 100 $\mu$M verapamil for 20 min at 37 °C. Unbound ligands were removed by ultracentrifugation and washing, and the samples were then UV-irradiated. The samples were promptly digested with trypsin (see Experimental Procedures) at varying trypsin-to-protein ratios (lane 1, 1:75; lane 2, 1:37.5; lane 3, 1:18.75; lane 4, 1:9.38; lane 5, 1:4.69; lane 6, 1:2.34; lane 7, 1:1.17) and photolabeled; trypsinized samples were separated by electrophoresis on a 10% SDS−polyacrylamide gel, transferred onto a nitrocellulose membrane, and subjected to autoradiography (B). The membrane was then analyzed by immunoblotting using mouse monoclonal anti-P-glycoprotein antibodies that recognize either the N-terminal half (MD13, C) or the C-terminal half (MD7, E) or both halves of P-gp (C219, G) to identify fragments corresponding to NBD1 or NBD2. The scans of the autoradiograph (B) and of the NBD-specific immunoblots (C, E) were colorized in green and red, respectively, using Adobe Photoshop. The photolabeled tryptic peptides immunoreactive with either MD13 or MD7 are seen in yellow color in (D) and (F), respectively. Some of the predicted structural features of P-gp, including the position of the protease-hypersensitive site, as well as the epitopes for MD13, MD7, and C219 are identified in (A).

A similar proteolytic cleavage experiment was carried out in the presence of V$_i$ (Figure 7). Results show that in the WT protein V$_i$ stimulates nucleotide trapping in both NBDs with a slight preference for NBD2, in agreement with previous results (*50*). In the presence of V$_i$, nucleotide trapping was seen in both NBD1 and NBD2 of the E552Q and E1197Q mutants (albeit at different ratios, depending on the position of the mutation). Control immunoblotting experiments with the C219 antibody indicate that the two Mdr3 halves are separated by the gel system and that lane 2 contains almost equal amounts of MD13 (NBD1) and MD7 (NBD2) immunoreactive species (data not shown). These results indicate that, in WT Mdr3 and the E552Q and E1197Q mutants, both NBDs can hydrolyze at least one
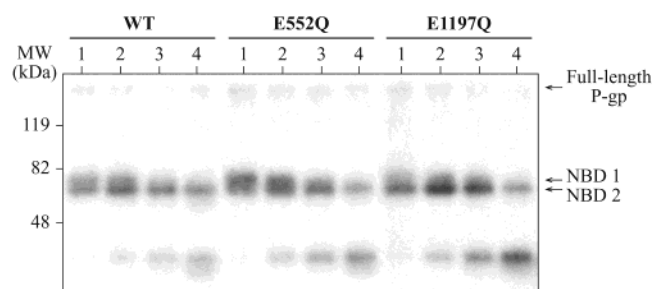
FIGURE 7:  Trypsin digestion of Mdr3 NB site mutants photolabeled with Mg-8-azido-[α-$^{32}$P]ATP in the presence of vanadate. Purified and activated wild-type and mutant Mdr3 variants were preincubated with 5 $\mu$M 8-azido-[α-$^{32}$P]ATP, 3 mM MgCl$_2$, and 100 $\mu$M verapamil in the presence of 200 $\mu$M vanadate for 20 min at 37 °C. Unbound ligands were removed by ultracentrifugation and washing, and the samples were then UV-irradiated. The samples were promptly digested with trypsin at varying trypsin-to-protein ratios (lane 1, 1:37.5; lane 2, 1:18.75; lane 3, 1:9.38; lane 4, 1:4.69). Photolabeled, trypsinized samples were separated by electrophoresis on 10% SDS−polyacrylamide gels, transferred onto nitrocellulose membranes, and subjected to autoradiography. The position of tryptic fragments corresponding to photolabeled NBD1 and NBD2 is indicated and was deduced by immunoblotting using MD13 and MD7 antibodies as described in the legend to Figure 6.

molecule of ATP with subsequent trapping of ADP in the presence of V$_i$ and inhibition.

## DISCUSSION

Several aspects of the mechanism of action of P-gp remain poorly understood; these include the exact catalytic cycle, the equivalent or nonequivalent nature of the NBDs for ATP binding and hydrolysis, and the type of signal produced at the NBDs by ATP hydrolysis that is transmitted to the drug-binding sites in the TMDs to mediate substrate efflux. We have previously identified glutamates E552 and E1197 in NBD1 and NBD2, respectively, of mouse Mdr3 as highly conserved carboxylate residues possibly involved in initiation or in other aspects of catalysis (*43*). These homologous residues map to the extended Walker B motif (or the D-loop) of the NBD and immediately follow the aspartate residues D551 and D1196, which coordinate Mg$^{2+}$ in the site. Multiple sequence alignments suggest that E552 and E1197 are homologous to E179 of the *Salmonella typhimurium* ABC transporter HisP. Crystallographic analysis of HisP strongly suggests that E179 positions a water molecule for in-line nucleophilic attack on the terminal phosphate of ATP (*34*). Indeed, E179 is mutation sensitive, and replacement to aspartate abrogates ATPase activity and transport activity (*34*). Therefore, it is highly likely that E552 and E1197 play a similar role in P-gp.

Results expressed in the present study suggest that the E552Q and E1197Q mutants are not completely inactive (as opposed to the Walker B mutant D551N) and that these mutants can indeed cleave ATP to ADP and P$_i$, undergoing partial reactions toward a full cycle of catalysis but never fully turning over. First, although neither mutant has ATPase activity that can be detected by P$_i$ release, both show V$_i$-induced trapping of 8-azido-[α-$^{32}$P]nucleotide that can be stimulated by drugs, a behavior clearly distinct from that of the D551N mutant. Previous studies have shown that hydrolysis of 8-azido-ATP to 8-azido-ADP is a prerequisite to V$_i$-induced trapping, resulting in the formation of a stable

{P-gp·Mg-8-azido-ADP·V$_i$} transition-state complex that can be cross-linked to the protein (*28*, *29*). Second, 8-azido-nucleotide trapping in the mutant enzymes in the absence and presence of V$_i$ is both temperature dependent and EDTA sensitive, as in the WT enzyme (Figure 2). Third, other transition-state analogues of P$_i$ can also support nucleotide trapping in the mutants, and this trapping is EDTA sensitive as well (Figure 3). Fourth, in the absence of V$_i$, nucleotide trapping takes place at the mutant NBD only (Figure 6). Finally, TLC analysis of the nucleotides bound to the enzymes following V$_i$ trapping of 8-azido-ATP shows formation of 8-azido-ADP by the WT and E552Q and E1197Q mutants (Figure 4). Together, these results indicate that E552Q and E1197Q can indeed cleave ATP to ADP and P$_i$ and that 8-azido-ADP is the nucleotide trapped in the photolabeled enzymes. Moreover, in their recent work, Sauna and colleagues also demonstrated using α- and γ-labeled 8-azido-[α-$^{32}$P]ATP that mutants at the equivalent positions of the human MDR1 protein (E556Q and E556A, E1201Q and E1201A, and the double mutants) are indeed capable of ATP hydrolysis and single-site catalysis (*59*). Therefore, in the E552Q and E1197Q mutants, steps downstream from the formation of the transition state, such as the release of MgADP and/or P$_i$, or others, must be impaired. The observation that similar amounts of 8-azido-[α-$^{32}$P]ADP are incorporated in the WT and mutant enzymes in the presence of V$_i$ under conditions of drug stimulation (*43*) strongly argues that P$_i$ release is normal and that another step downstream of P$_i$ release is impaired in the mutant enzymes. The finding that in the absence of V$_i$ nucleotide trapping (ADP) occurs in the mutant NBD exclusively supports the contention that ADP release from the mutant NBD is the key catalytic step impaired in the mutant enzymes. Although our interpretation favors ADP release as the mechanistic step impaired in the mutants, the work by Sauna and colleagues (*59*) suggests that ADP release is impaired only in the double mutants but not in the single mutants. Indeed, they suggest that the single E556A/Q and E1202A/Q mutants are defective in the second ATP hydrolysis event of the catalytic cycle, which should reset the protein after hydrolysis at the first site. Additional experiments will be required to determine whether ADP release is in fact occurring in the mouse Mdr3 mutants described in the present report.

The question of whether NBD1 and NBD2 of P-gp are structurally and functionally equivalent and whether they play distinct roles during catalysis and transport is still being debated. In support of functional equivalence of the two sites are the observations that (1) there is no evidence for binding site heterogeneity in ATP- and ADP-binding studies with purified P-gp (*60*, *61*), (2) mutations in Walker A or B residues in either NBD completely abolish drug transport and ATPase activity (*25*, *49*), (3) each P-gp half shows low intrinsic ATPase activity (*27*), (4) V$_i$ inhibits ATP hydrolysis and can induce trapping of 8-azido-[α-$^{32}$P]ADP·V$_i$ in P-gp with seemingly equal labeling of NBD1 and NBD2 (*28*, *29*, *32*), and (5) NEM inhibits P-gp ATPase activity by binding to a cysteine present in the Walker A motif of NBD1 and NBD2 (*61*, *62*), and NEM-sensitive ATPase activity is inhibited by similar ATP concentrations in single-cysteine P-gp mutants in NBD1 and NBD2 (*26*). Opposing data in support of structurally and functionally distinct NBDs include

the observations that (1) under binding conditions (4 °C), 8-azido-[$\alpha$-$^{32}$P]ATP preferentially labels NBD1, while under hydrolysis conditions (37 °C and $V_i$), NBD2 is preferentially labeled in P-gp (*50*), (2) equivalent mutations in Walker B residues of NBD1 and NBD2 (D551N, D1196N) cause different conformational changes in Mdr3 as measured by trypsin sensitivity (*58*), (3) median inhibition of ATPase activity in cysteine-less P-gp mutants bearing single-cysteine replacements in NBD1 or NBD2 occurs at different NEM concentrations (*26*), and (4) functional studies of CFTR (*63–66*), of MRP1 (*67–71*), and of the NBDs of the bacterial arsenite transporter ArsA (*72*) show that NBD1 and NBD2 have different ATP-binding and hydrolysis properties. The study of E552Q and E1197Q reported here clearly argues in favor of two NBDs that are not functionally equivalent in full-length P-gp. This is most clearly illustrated by results from the $V_i$ dose–response experiment (Figure 5). In this experiment it can be observed that E552Q and E1197Q trap nucleotide in the absence of $V_i$ and that the response of each mutant to $V_i$ is completely different, with E552Q showing a strongly dose-dependent increase in labeling (similar to WT), while $V_i$ has little effect on nucleotide trapping in E1197Q. This behavior is inconsistent with the presence of two functionally equivalent NBDs in the protein. Since nucleotide trapping in the mutants occurs after cleavage of ATP (with ADP trapped; see above), the differential $V_i$ dose–response observed in E552Q and E1197Q is most easily explained by differential sensitivity of the nonmutant site to inhibition by $V_i$. Finally, proteolytic cleavage studies of photolabeled WT and mutant proteins have shown that (a) in the absence of $V_i$, only the mutant NBD is occluded, and (b) in the presence of $V_i$, both NBDs are occluded (albeit at a different degree; Figure 7). The idea of asymmetrical NBDs in P-gp is in agreement with the results previously reported by Hrycyna et al. (*50*) and Aleksandrov et al. (*64–66*), and the results in this study are reminiscent of parallel studies of MRP1 (*67–71*) that also suggest nonequivalence of the two NBDs since it was observed for MRP1 that (1) mutation at the Walker A lysine of NBD2 has a more severe effect on transport than the homologous mutation at NBD1, (2) there is preferential binding of 8-azido-[$\gamma$-$^{32}$P]ATP at NBD1, (3) there is preferential $V_i$-induced trapping of 8-azido-[$\alpha$-$^{32}$P]-nucleotide at NBD2, and (4) NBD2 is also preferentially labeled by 8-azido-[$\alpha$-$^{32}$P]ADP.

In summary, the present work supports the finding that both NBDs are essential for function with complete cooperativity between the two sites and suggests that the E552 and E1197 residues of mouse Mdr3 are probably not the catalytic residues, as the E552Q and E1197Q mutants can hydrolyze ATP in both nucleotide-binding domains. Furthermore, our results support a model in which the two NBDs of P-gp are not functionally equivalent.

## ACKNOWLEDGMENT

## REFERENCES

1. Gottesman, M. M., Fojo, T., and Bates, S. E. (2002) *Nat. Rev. Cancer 2*, 48–58.
2. Gottesman, M. M. (2002) *Annu. Rev. Med. 53*, 615–627.
3. Gottesman, M. M., and Ambudkar, S. V. (2001) *J. Bioenerg. Biomembr. 33*, 453–458.
4. Gros, P., Croop, J., and Housman, D. (1986) *Cell 47*, 371–380.
5. Chen, C. J., Chin, J. E., Ueda, K., Clark, D. P., Pastan, I., Gottesman, M. M., and Roninson, I. B. (1986) *Cell 47*, 381–389.
6. Linton, K. J., and Higgins, C. F. (1998) *Mol. Microbiol. 28*, 5–13.
7. Loo, T. W., and Clarke, D. M. (1995) *J. Biol. Chem. 270*, 843–848.
8. Kast, C., Canfield, V., Levenson, R., and Gros, P. (1996) *J. Biol. Chem. 271*, 9240–9248.
9. Chang, G., and Roth, C. B. (2001) *Science 293*, 1793–1800.
10. Safa, A. R. (1993) *Cancer Invest. 11*, 46–56.
11. Buschman, E., and Gros, P. (1991) *Mol. Cell. Biol. 11*, 595–603.
12. Zhou, Y., Gottesman, M. M., and Pastan, I. (1999) *Mol. Cell. Biol. 19*, 1450–1459.
13. Devine, S. E., Ling, V., and Melera, P. W. (1992) *Proc. Natl. Acad. Sci. U.S.A. 89*, 4564–4568.
14. Choi, K. H., Chen, C. J., Kriegler, M., and Roninson, L. B. (1988) *Cell 53*, 519–529.
15. Shustik, C., Dalton, W., and Gros, P. (1995) *Mol. Aspects Med. 16*, 1–78.
16. Loo, T. W., and Clarke, D. M. (1999) *Biochim. Biophys. Acta 1461*, 315–325.
17. Loo, T. W., and Clarke, D. M. (1999) *J. Biol. Chem. 274*, 35388–35392.
18. Ambudkar, S. V., Lelong, I. H., Zhang, J., Cardarelli, C. O., Gottesman, M. M., and Pastan, I. (1992) *Proc. Natl. Acad. Sci. U.S.A. 89*, 8472–8476.
19. Sarkadi, B., Price, E. M., Boucher, R. C., Germann, U. A., and Scarborough, G. A. (1992) *J. Biol. Chem. 267*, 4854–4858.
20. al-Shawi, M. K., and Senior, A. E. (1993) *J. Biol. Chem. 268*, 4197–4206.
21. Sharom, F. J., Yu, X., and Doige, C. A. (1993) *J. Biol. Chem. 268*, 24197–24202.
22. Senior, A. E., al-Shawi, M. K., and Urbatsch, I. L. (1995) *FEBS Lett. 377*, 285–289.
23. Ambudkar, S. V., Cardarelli, C. O., Pashinsky, I., and Stein, W. D. (1997) *J. Biol. Chem. 272*, 21160–21166.
24. Shapiro, A. B., and Ling, V. (1994) *J. Biol. Chem. 269*, 3745–3754.
25. Azzaria, M., Schurr, E., and Gros, P. (1989) *Mol. Cell. Biol. 9*, 5289–5297.
26. Loo, T. W., and Clarke, D. M. (1995) *J. Biol. Chem. 270*, 22957–22961.
27. Loo, T. W., and Clarke, D. M. (1994) *J. Biol. Chem. 269*, 7750–7755.
28. Urbatsch, I. L., Sankaran, B., Weber, J., and Senior, A. E. (1995) *J. Biol. Chem. 270*, 19383–19390.
29. Urbatsch, I. L., Sankaran, B., Bhagat, S., and Senior, A. E. (1995) *J. Biol. Chem. 270*, 26956–26961.
30. Sauna, Z. E., and Ambudkar, S. V. (2000) *Proc. Natl. Acad. Sci. U.S.A. 97*, 2515–2520.
31. Ramachandra, M., Ambudkar, S. V., Chen, D., Hrycyna, C. A., Dey, S., Gottesman, M. M., and Pastan, I. (1998) *Biochemistry 37*, 5010–5019.
32. Sauna, Z. E., and Ambudkar, S. V. (2001) *J. Biol. Chem. 276*, 11653–11661.
33. Walker, J. E., Saraste, M., Runswick, M. J., and Gay, N. J. (1982) *EMBO J. 1*, 945–951.
34. Hung, L. W., Wang, I. X., Nikaido, K., Liu, P. Q., Ames, G. F., and Kim, S. H. (1998) *Nature 396*, 703–707.
35. Diederichs, K., Diez, J., Greller, G., Muller, C., Breed, J., Schnell, C., Vonrhein, C., Boos, W., and Welte, W. (2000) *EMBO J. 19*, 5951–5961.
36. Yuan, Y. R., Blecker, S., Martsinkevich, O., Millen, L., Thomas, P. J., and Hunt, J. F. (2001) *J. Biol. Chem. 276*, 32313–32321.
37. Karpowich, N., Martsinkevich, O., Millen, L., Yuan, Y. R., Dai, P. L., MacVey, K., Thomas, P. J., and Hunt, J. F. (2001) *Structure 9*, 571–586.
38. Hopfner, K. P., Karcher, A., Shin, D. S., Craig, L., Arthur, L. M., Carney, J. P., and Tainer, J. A. (2000) *Cell 101*, 789–800.
39. Wiley, D. C., and Gaudet, R. (2001) *EMBO J. 20*, 4964–4972.
40. Locher, K. P., Lee, A. T., and Rees, D. C. (2002) *Science 296*, 1091–1098.

41. Kranitz, L., Benabdelhak, H., Horn, C., Blight, M. A., Holland, I. B., and Schmitt, L. (2002) *Acta Crystallogr., Sect. D: Biol. Crystallogr. 58*, 539−541.

42. Smith, P. C., Karpowich, N., Millen, L., Moody, J. E., Rosen, J., Thomas, P. J., and Hunt, J. F. (2002) *Mol. Cell 10*, 139−149.

43. Urbatsch, I. L., Julien, M., Carrier, I., Rousseau, M. E., Cayrol, R., and Gros, P. (2000) *Biochemistry 39*, 14138−14149.

44. Lerner-Marmarosh, N., Gimi, K., Urbatsch, I. L., Gros, P., and Senior, A. E. (1999) *J. Biol. Chem. 274*, 34711−34718.

45. Van Veldhoven, P. P., and Mannaerts, G. P. (1987) *Anal. Biochem. 161*, 45−48.

46. Bruggemann, E. P., Germann, U. A., Gottesman, M. M., and Pastan, I. (1989) *J. Biol. Chem. 264*, 15483−15488.

47. Shapiro, A. B., Duthie, M., Childs, S., Okubo, T., and Ling, V. (1996) *Int. J. Cancer 67*, 256−263.

48. Laemmli, U. K. (1970) *Nature 227*, 680−685.

49. Urbatsch, I. L., Beaudet, L., Carrier, I., and Gros, P. (1998) *Biochemistry 37*, 4592−4602.

50. Hrycyna, C. A., Ramachandra, M., Germann, U. A., Cheng, P. W., Pastan, I., and Gottesman, M. M. (1999) *Biochemistry 38*, 13887−13899.

51. Beaudet, L., Urbatsch, I. L., and Gros, P. (1998) *Biochemistry 37*, 9073−9082.

52. Horio, M., Gottesman, M. M., and Pastan, I. (1988) *Proc. Natl. Acad. Sci. U.S.A. 85*, 3580−3584.

53. Sauna, Z. E., Smith, M. M., Muller, M., and Ambudkar, S. V. (2001) *J. Biol. Chem. 276*, 21199−21208.

54. Fisher, A. J., Smith, A. C., Thoden, J. B., Smith, R., Sutoh, K., Holden, H. M., and Rayment, I. (1995) *Biochemistry 34*, 8960−8972.

55. Smith, C. A., and Rayment, I. (1996) *Biochemistry 35*, 5404−5417.

56. Sankaran, B., Bhagat, S., and Senior, A. E. (1997) *Arch. Biochem. Biophys. 341*, 160−169.

57. Sankaran, B., Bhagat, S., and Senior, A. E. (1997) *Biochemistry 36*, 6847−6853.

58. Julien, M., and Gros, P. (2000) *Biochemistry 39*, 4559−4568.

59. Sauna, Z. E., Muller, M., Peng, X.-H., and Ambudkar, S. V. (2002) *Biochemistry 41*, 13989−14000.

60. Urbatsch, I. L., Gimi, K., Wilke-Mounts, S., and Senior, A. E. (2000) *J. Biol. Chem. 275*, 25031−25038.

61. Sharom, F. J., Liu, R., Romsicki, Y., and Lu, P. (1999) *Biochim. Biophys. Acta 1461*, 327−345.

62. al-Shawi, M. K., Urbatsch, I. L., and Senior, A. E. (1994) *J. Biol. Chem. 269*, 8986−8992.

63. Szabo, K., Szakacs, G., Hegeds, T., and Sarkadi, B. (1999) *J. Biol. Chem. 274*, 12209−12212.

64. Aleksandrov, L., Mengos, A., Chang, X., Aleksandrov, A., and Riordan, J. R. (2001) *J. Biol. Chem. 276*, 12918−12923.

65. Aleksandrov, L., Aleksandrov, A. A., Chang, X. B., and Riordan, J. R. (2002) *J. Biol. Chem. 277*, 15419−15425.

66. Powe, A. C., Jr., Al-Nakkash, L., Lin, M., and Hwang, T.-C. (2002) *J. Physiol. 5392*, 333−346.

67. Gao, M., Cui, H. R., Loe, D. W., Grant, C. E., Almquist, K. C., Cole, S. P., and Deeley, R. G. (2000) *J. Biol. Chem. 275*, 13098−13108.

68. Nagata, K., Nishitani, M., Matsuo, M., Kioka, N., Amachi, T., and Ueda, K. (2000) *J. Biol. Chem. 275*, 17626−17630.

69. Hou, Y., Cui, L., Riordan, J. R., and Chang, X. (2000) *J. Biol. Chem. 275*, 20280−20287.

70. Cui, L., Hou, Y. X., Riordan, J. R., and Chang, X. B. (2001) *Arch. Biochem. Biophys. 392*, 153−161.

71. Hou, Y. X., Cui, L., Riordan, J. R., and Chang, X. B. (2002) *J. Biol. Chem. 277*, 5110−5119.

72. Zhou, T., and Rosen, B. P. (1997) *J. Biol. Chem. 272*, 19731−19737.